Formation of an Unfolding Intermediate State of Soluble Chloride Intracellular Channel Protein CLIC1 at Acidic pH[†]

Sylvia Fanucchi, Roslin J. Adamson, and Heini W. Dirr*

Protein Structure-Function Research Unit, School of Molecular and Cell Biology, University of the Witwatersrand, Johannesburg 2050, South Africa

Received June 19, 2008; Revised Manuscript Received September 10, 2008

ABSTRACT: CLIC proteins function as anion channels when their structures convert from a soluble form to an integral membrane form. While very little is known about the mechanism of the conversion process, channel formation and activity are highly pH-dependent. In this study, the structural properties and conformational stability of CLIC1 were determined as a function of pH in the absence of membranes to improve our understanding of how its conformation changes when the protein encounters the acidic environment at the surface of a membrane. Although the global conformation and size of CLIC1 are not significantly altered by pH in the range of 5.5−8.2, equilibrium unfolding studies reveal that the protein molecule becomes destabilized at low pH, resulting in the formation of a highly populated intermediate with a solvent-exposed hydrophobic surface. Unlike the intermediates formed by many soluble pore-forming proteins for their insertion into membranes, the CLIC1 intermediate is not a molten globule. Acid-induced destabilization and partial unfolding of CLIC1 involve helix α1 which is the major structural element of the transmembrane region. We propose that the acidic environment encountered by CLICs at the surface of membranes primes the transmembrane region in the N-domain, thereby lowering the energy barrier for the conversion of soluble CLICs to their membrane-inserted forms.

Chloride intracellular channels (CLICs)[1] belong to a family of acidic anion channel proteins that are widely distributed in tissues and cells (*1*−*5*). CLICs are expressed as soluble proteins without a leader sequence for membrane targeting. They can, however, insert into plasma and intracellular membranes, where they perform their channel functions in a variety of biological processes (*6*). Solution-to-membrane partitioning has been demonstrated in vitro with only recombinant CLICs and synthetic membranes, suggesting that membrane binding and insertion are not receptor-mediated. The CLIC family consists of seven members whose sequences are highly conserved across species [CLIC1, CLIC2, CLIC3, CLIC4, and CLIC5A (all with approximately 240 amino acids)] and two larger variants, CLIC5B and CLIC6, that contain additional unrelated N-terminal domains that are not evolutionarily conserved (*6*).

Crystallographic data indicate that the structure of soluble CLICs shares a common fold that is related to the canonical fold of the soluble glutathione transferases (GSTs) (*7*−*12*).

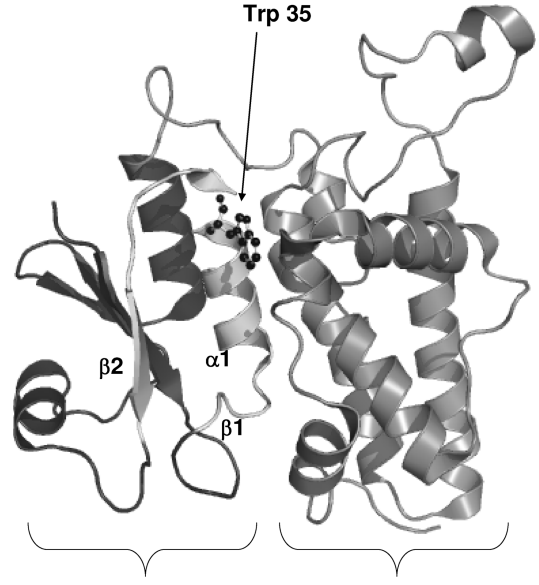

FIGURE 1: Crystal structure of reduced CLIC1. The N-terminal domain containing the thioredoxin fold is colored black, and the all α-helical C-terminal domain is colored gray. The single tryptophan residue, Trp35, is shown. The helix that is considered likely to traverse the membrane is composed of β-strand 1, α-helix 1, and β-strand 2 is highlighted in white in the figure. The figure was rendered with PyMol (*60*) using PDB entry 1k0m (*8*).

While soluble CLICs are monomeric, the GSTs are dimeric and do not insert into membranes. The GST-like fold of CLIC proteins consists of two domains (Figure 1): a thioredoxin-like N-domain and a larger all-helical C-domain.

[†] This work was supported by the University of the Witwatersrand, South African National Research Foundation Grant 205359, and the South African Research Chairs Initiative of the Department of Science and Technology and National Research Foundation Grant 64788.

* To whom correspondence should be addressed. Telephone: +27 11 7176352. Fax: +27 11 7176351. E-mail: heinrich.dirr@wits.ac.za.

[1] Abbreviations: ANS, 8-anilino-1-naphthalene sulfonate; CLIC, chloride intracellular channel; DLS, dynamic light scattering; DTT, dithiothreitol; E_{222}, ellipticity measured at 222 nm; F_{345}, fluorescence intensity at 345 nm; F_{max}, maximum intensity of the fluorescence emission spectrum; far-UV CD, far-ultraviolet circular dichroism; GST, glutathione transferase; λ_{max}, wavelength at which the fluorescence spectra show maximum emission; near-UV CD, near-ultraviolet circular dichroism.

10.1021/bi801147r CCC: $40.75
Published on Web 10/14/2008

The role of the C-domain is unknown, although its function appears to be conserved in all members of the GST superfamily (*10*). There is substantial evidence demonstrating that the amino acid sequence corresponding to the amphipathic $\beta1\alpha1\beta2$ motif in the thioredoxin-like N-domain of soluble CLICs forms the transmembrane region (*2, 8, 10, 13*−*16*) (Figure 1). The transmembrane region has been shown to span membranes (*17, 18*), and while its conformation in the membrane is unknown, it is likely to be helical (*19, 20*). The transmembrane regions of at least four CLICs have been proposed to associate in the membrane to form a functional pore (*21*). However, the conformational changes that these proteins undergo to bind to and penetrate membranes, and how and when they multimerize to achieve channel formation, are unknown. For the supersecondary $\beta1\alpha1\beta2$ structural motif to function as a transmembrane region, it must detach from the C-domain of soluble CLIC1, extend, and refold into its new membrane-insertable conformation.

CLIC channel formation and activity have been demonstrated to be highly pH-dependent in that low pH values facilitate the appearance of CLIC channels in artificial membranes (*10, 13, 22*). The acidic pH at the surface of a membrane (*23, 24*) can function to prime the structure of a soluble protein which lowers the activation energy barrier for its conversion to a membrane-insertable conformation (*24*−*26*). Acid-induced destabilization and conformational changes have been demonstrated for many bacterial pore-forming toxins (*27*−*30*) and for some other proteins (*31, 32*). An acid-induced formation of a molten globule-like intermediate appears to be a major mechanism for the membrane insertion of numerous soluble proteins (*24, 33*−*37*). The loose tertiary structure of a molten globule state enhances the exposure of hydrophobic patches to solvent, making the exchange of protein−protein interactions with protein−lipid interactions energetically more favorable, thus facilitating membrane insertion (*38*). However, a molten globule intermediate may not be essential for all proteins that adopt both solution and membrane conformations, as shown for anti-apoptotic protein Bcl-x_L (*31*). The conversion to its membrane conformation requires both acidic conditions and the presence of membranes and appears to be driven by the protonation of acidic side chains (*31, 39, 40*).

Given that very little is known about the mechanism by which CLICs convert from a soluble form to a membrane-inserted form and that there are striking structural differences between CLICs and other soluble-to-membrane proteins, the conformational stability of soluble, reduced CLIC1 was investigated as a function of pH in the absence of membranes. The goal was to improve our understanding of how the protein's conformation might change as it encounters the acidic environment at the surface of a membrane and to characterize the conformational transitions associated with its functional properties.

EXPERIMENTAL PROCEDURES

Materials. Isopropyl β-D-thiogalactoside (IPTG) and dithiothreitol (DTT) were acquired from Inqaba Biotech (Pretoria, South Africa). Ultrapure urea was purchased from Merck laboratory supplies (Darmstadt, Germany). 8-Anilino-1-naphthalene sulfonate (ANS), lysozyme, and bovine thrombin were obtained from Sigma-Aldrich (St. Louis, MO). All other chemicals used were of standard analytical grade.

Methods. CLIC1 Expression and Purification. CLIC1 was purified from a batch culture of BL21(DE3) *Escherichia coli* cells transformed with the pGEX-4T-1 plasmid following the general protocol of Tulk and Edwards (*17*). The pGEX-4T-1 plasmid that encodes the GST−CLIC1 fusion protein in *E. coli* (*41*) was a gift from S. N. Breit (Centre for Immunology, St. Vincent's Hospital and University of New South Wales, Sydney, Australia).

The fusion protein was incubated with 20 units of bovine thrombin per liter of culture for 16 h at 20 °C. CLIC1 and thrombin were separated using DEAE anion-exchange chromatography at pH 6.0. CLIC1 was recovered from the DEAE Sepharose column with 300 mM NaCl (pH 7.0). Approximately 20 mg of CLIC1 was purified per liter of culture. The purified protein was exchanged into storage buffer [50 mM Na_2HPO_4, 0.02% NaN_3, and 1 mM DTT (pH 7.0)].

Dynamic Light Scattering. Measurements were performed on a Zetasizer Nano-S light scattering device with the laser set at 633 nm (Malvern). The solutions were filtered (0.1 μm) before measurement. Measurements were performed at 20 °C.

Spectroscopic Methods. Far-UV CD measurements were performed on a Jasco model 810 CD spectropolarimeter. Averaged CD signals, corrected for solvent, were converted to mean residue ellipticity [Θ] (degrees square centimeters per decimole per residue); $[\Theta] = (100\theta)/(Cnl)$, where C is the protein concentration (millimolar), θ is the measured ellipticity (millidegrees), n is the number of residues, and l is the path length (centimeters).

Fluorescence measurements were conducted using a Perkin-Elmer LS50B luminescence spectrometer. The intrinsic fluorescence of CLIC1 was monitored by exciting the single tryptophan residue (Trp35) and the eight tyrosine residues at 280 nm. Slit widths of 5 nm were used. The binding of the anionic dye, ANS, to CLIC1 was monitored by fluorescence enhancement using an excitation wavelength of 390 nm and an emission wavelength of 460 nm. Dynamic acrylamide quenching of the single tryptophan residue employed a modified form of the Stern−Volmer equation:

$$\frac{F_0}{F} = (1 + K_{sv}[Q])e^{V[Q]}$$

where F_0 and F are fluorescence intensities at 345 nm in the absence and presence of quencher, respectively, K_{sv} is the collisional quenching constant, V is the static quenching constant, and [Q] is the concentration of acrylamide. The protein in the presence of acrylamide was excited at 295 nm, and emission was measured at 345 nm for the native state and at 340 nm for the intermediate state. Slit widths of 6 nm were used.

Urea-Induced Equilibrium Unfolding. The unfolding of CLIC1 (2 μM) in 0−8 M urea was followed by far-UV CD, fluorescence, ANS binding, and light scattering. The solutions were left for 2 h at 20 °C to allow them to reach equilibrium. Reversibility was established prior to fitting the data.

Data Analysis. Unfolding data were globally fit (*42*) to either a two-state monomer (N ↔ U) or a three-state monomer (N ↔ I ↔ U) model using Savuka version 6.2.26 (*43, 44*). The thermodynamic parameters, $\Delta G(H_2O)$ and m value, obtained from the global fits [using the linear

extrapolation method (*45, 46*)] were used to calculate the fractional populations of each species from the equilibrium constants.

RESULTS

Conformational Stability of CLIC1 as a Function of pH. Prior to membrane insertion, soluble CLIC1 will move from a neutral pH in the cytosol to an acidic environment at the membrane surface where it is prepared for membrane insertion. Further, given that the cytosol is highly reducing, soluble CLICs are unlikely to exist in an oxidized form (*14*). Therefore, to understand better how the structure of CLIC1 is primed for membrane insertion, the conformational stability of soluble, reduced CLIC1 was measured at pH 7.0 and 5.5 in the absence of membranes by far-UV CD and tryptophan fluorescence.

CLIC1 displays a far-UV CD spectrum (Figure 2A) that is typical of a predominantly α-helical protein, consistent with crystallized CLIC1 which has 45% of its sequence in α-helices and 10% in β-strands (*8*). Ellipticity data shown in Figures 2A and 3 indicate that the secondary structure remains essentially unchanged between pH 6 and 7.5. There is greater variance at pH <6, although the slight decrease in ellipticity observed at 222 nm at the low pH values appears to be significant within error. A pH of 5.5−7.5 has little effect on the tertiary environment of the only tryptophan residue in CLIC1, Trp35 (Figures 2B and 3). A fluorescence maximum emission wavelength at ∼345 nm indicates a partially buried Trp35, as observed in the crystal structure (*8*). Dynamic light scattering data show that the size of soluble CLIC1 remains unchanged at pH 5.5−7.5, corresponding to the monomeric form of the protein (Figure 3).

CLIC1 unfolds reversibly at both pH 7 and 5.5 and displays no hysteresis, as demonstrated by the superimposable unfolding and refolding transitions at pH 7 (Figure 4). The independence of the unfolding transitions from protein concentration (1 to 10 μM) indicates that unfolding involves only monomeric CLIC1 species (Figure S1 of the Supporting Information). Light scattering data indicated that protein aggregation was negligible throughout the unfolding transitions (Figure S2 of the Supporting Information).

The dependence of CLIC1 unfolding upon pH is shown in Figure 5. At pH 7.0, unfolding is characterized by monophasic transitions. All spectroscopic changes (ellipticity and fluorescence) shown in Figure 5A coincide with a C_m at 4.8 M urea, indicating a simultaneous loss of secondary structure and the tertiary environment of Trp35. This behavior is highly suggestive of a cooperative two-state process, N ↔ U, where N and U are folded and unfolded CLIC1, respectively. The unfolding data at pH 7.0 fit best to a two-state model. The global fit of the fluorescence and CD data shown in Figure 5A gives a $\Delta G(H_2O)$ of 9.5 ± 0.6 kcal/mol and an m value of 2.0 ± 0.1 kcal mol^{-1} (M urea)$^{-1}$. The reduced χ^2 for the fit is 0.25, and the goodness of fit is 1.

At pH 5.5, a condition that the soluble protein would encounter near or at the surface of membranes (*23, 24, 37*), the unfolding behavior of CLIC1 changes dramatically. The fluorescence data show wavelength-dependent changes that are inconsistent with two-state behavior (Figure 5B). Furthermore, the spectroscopic data monitored by CD and fluorescence no longer coincide (Figure 5B). Equilibrium

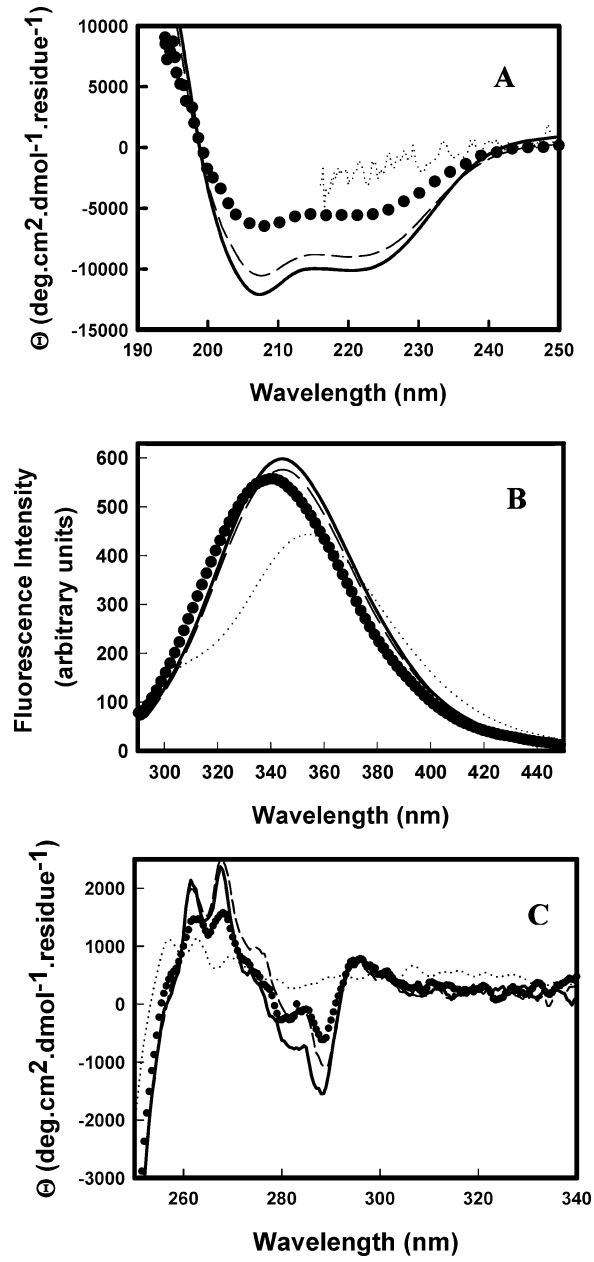

FIGURE 2: Far-UV circular dichroism spectra (A), fluorescence emission spectra (B), and near-UV circular dichroism spectra (C) of 5 μM CLIC1 (A and B) or 60 μM CLIC1 (C) recorded on native protein at pH 7.0 (—) and 5.5 (– – –). Spectra for the denatured state (8 M urea) (•••) and the intermediate state (pH 5.5 with 3.8 M urea) (●) are also shown. The far-UV CD spectra show minima at 208 and 222 nm which are characteristic of an α-helical protein. CLIC1 loses ∼30% of its secondary structure upon formation of the intermediate. The emission spectra at pH 7.0 and 5.5 peak at ∼345 nm, while the intermediate state shows a blue-shifted emission spectrum.

unfolding of CLIC1 at pH 5.5 therefore cannot be described by a two-state N ↔ U model. The monophasic curves (fluorescence at wavelengths greater than 345 nm) and the biphasic curves (E222 and fluorescence at wavelengths less than 345 nm) were globally fit to a three state model, N ↔ I ↔ U, where I is an intermediate (Figure 5B). The free energy of formation of the intermediate at pH 5.5 is 7.5 ± 0.5 kcal/mol with an m value of 2.2 ± 0.2 kcal mol^{-1} (M urea)$^{-1}$, and the free energy of unfolding of the intermediate is 16.8 ± 1.8 kcal/mol with an m value of 4.0 ± 0.4 kcal mol^{-1} (M urea)$^{-1}$. This suggests that the formation of the

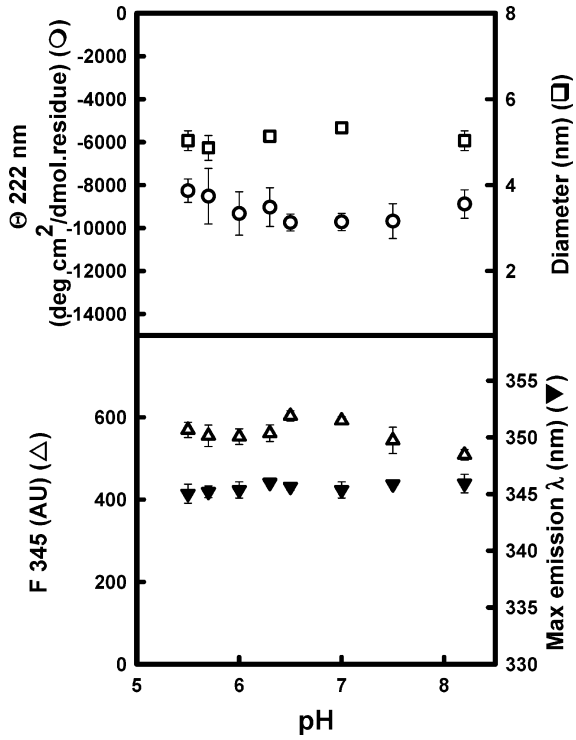

FIGURE 3: pH dependence of the mean residue ellipticity at 222 nm (○), the hydrodynamic diameter (□), the fluorescence intensity at 345 nm (△), and the wavelength of maximum fluorescence emission (▼) of CLIC1.

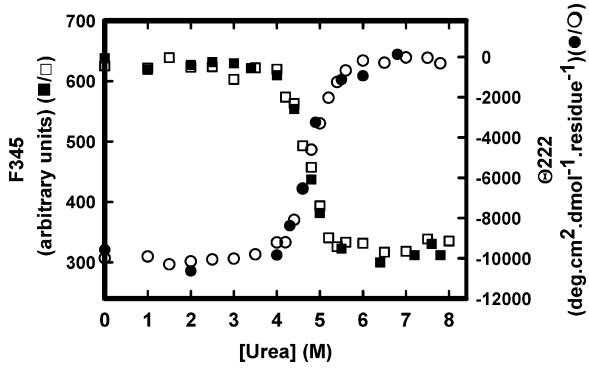

FIGURE 4: Unfolding (○ and □) and refolding (● and ■) transitions of CLIC1 at pH 7.0 when monitored by CD ellipticity at 222 nm (○ and ●) and fluorescence emission at 345 nm (□ and ■).

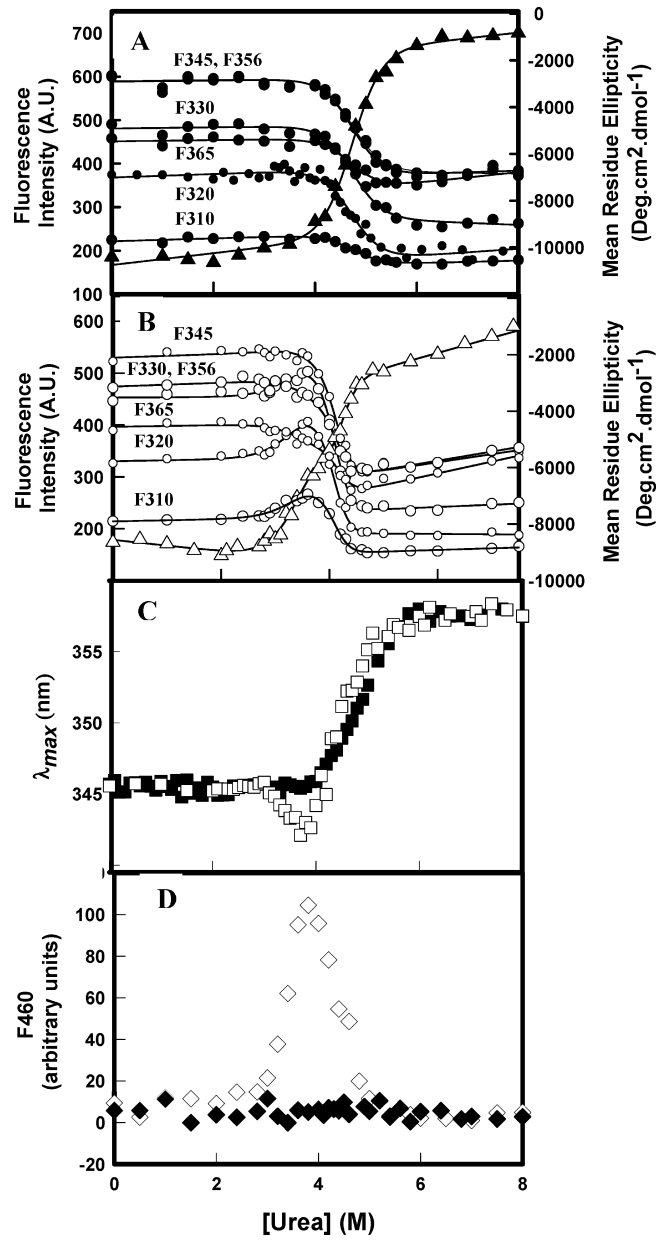

FIGURE 5: Equilibrium unfolding of CLIC1 at pH 7 (filled) and 5.5 (empty) as monitored by ellipticity at 222 nm (▲ and △) and fluorescence intensity at various wavelengths (● and ○). The lines represent the best global fits of a two-state (A) and three-state (B) model to the data. The wavelength of maximum fluorescence emission (■ and □) and binding of 200 μM ANS (◇ and ◆) are represented as a function of urea concentration in panels C and D, respectively. Experiments were conducted at 20 °C with 2 μM CLIC1.

intermediate is energetically favorable under these conditions. The data fit best to a three-state model and have a reduced χ^2 of 0.25 and a goodness of fit 1. The three-state model is further supported by binding studies with ANS, a fluorescent dye widely used to detect hydrophobic patches in proteins and/or unfolding intermediates (*47, 48*). The data in Figure 5D show that native and unfolded CLIC1 do not bind ANS and that no binding of ANS is observed at any point along the unfolding transition at pH 7.0. However, at pH 5.5, an ANS binding peak appears between 3.0 and 4.8 M urea (Figure 5D). The ascending limb of the peak corresponds to the initial loss of secondary structure (~50%) and the blue shift in the maximum emission wavelength of Trp35 (Figures 2B and 5C). A further decrease in the level of secondary structure (>3.8 M urea) coincides with the decrease in the fluorescence intensity of Trp35.

Unfolding studies were also performed at a higher temperature (37 °C) to determine whether the intermediate state could also be populated at pH 7. When unfolded with urea at 37 °C, which is well below the temperature at which CLIC1 begins to melt, the protein behaves in a way that is similar to that when it is unfolded at pH 5.5 and 20 °C (Figure S3 of the Supporting Information), indicative of the formation of an intermediate. The spectroscopic and ANS binding behavior of this intermediate are the same as those of the intermediate formed during the unfolding of CLIC1 at pH 5.5 and 20 °C.

Properties of the Unfolding Intermediate. The intermediate is most highly populated at 3.8 M urea and pH 5.5 (Figure 6). It is more highly populated than both the native and unfolded states under these conditions. The secondary

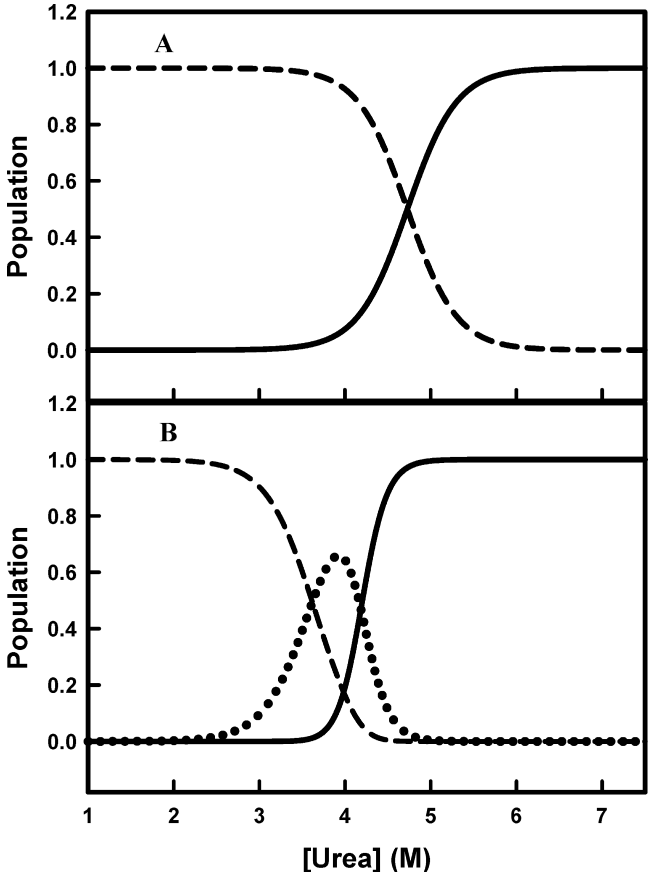

FIGURE 6: Fractional populations of the native (– – –), unfolded (—), and intermediate states (•••) as a function of urea concentration. The populations were calculated using the thermodynamic parameters obtained from globally fitting the data to a two-state model at pH 7 (A) and to a three-state model at pH 5.5 (B).

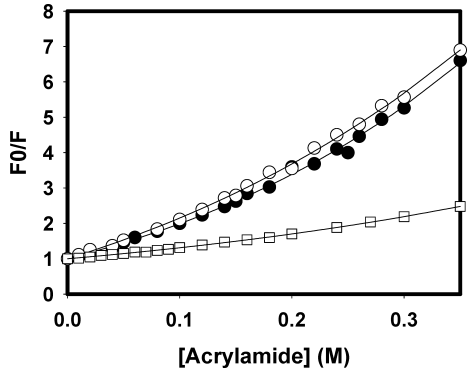

FIGURE 7: Quenching of the fluorescence of Trp35 in CLIC1 by acrylamide. Experiments were performed at pH 7 (●) and 5.5 (○) and on the intermediate state (pH 5.5 with 3.8 M urea) (□).

structure of the unfolding intermediate is mainly α-helical and retains ~50% of the native structure of CLIC1 at pH 5.5 (Figure 2A). The blue shift in the fluorescence spectrum (Figure 2B) indicates that during the formation of the intermediate, Trp35 moves into a more hydrophobic environment. This is accompanied by a significant decrease in the accessibility of Trp35 to quenching by acrylamide, as shown by the Stern−Volmer plots in Figure 7. The static and dynamic quenching constants are reported in Table 1. The intermediate possesses a well-packed tertiary structure, as seen by its near-UV CD spectrum relative to that of the native state (Figure 2C), with exposed hydrophobic sites to which the fluorescent dye ANS binds (K_d = 20 μM) (Figure 8, inset). The hydrophobic nature of the binding sites is demonstrated by the significant blue shift (from 520 nm in water to 460 nm) and enhanced intensity of the fluorescence spectrum of intermediate-bound ANS (Figure 8). Further, the intermediate unfolds cooperatively at high concentrations of urea, consistent with the presence of significant tertiary interactions. Together, these properties of the intermediate state of CLIC1 are inconsistent with a molten globule-like state. Molten globule proteins typically display a poorly defined tertiary structure, bind ANS weakly (millimolar range), and unfold noncooperatively at low concentrations of denaturant (*49*−*55*). While many other membrane-insertable proteins, particularly protein toxins, are reported to form an acid-induced molten globule state (*20, 24, 33*−*36*), this is not the case for CLIC1 and Bcl (*31*).

Table 1: pH and Urea Dependence of Static (V) and Dynamic (K_{sv}) Acrylamide Quenching Constants for CLIC1

	K_{sv} (M^{-1})	V (M^{-1})
0 M urea at pH 7	7.0	1.7
0 M urea at pH 5.5	8.6	1.6
3.8 M urea at pH 5.5	2.2	1.5

DISCUSSION

Water-soluble proteins that insert into membranes follow a multistep process that includes a pH-dependent structural reorganization that enables them to partition into lipid bilayers (*20*). Very little, however, is known about how soluble CLICs convert to their membrane-inserted forms which function as anionic channel proteins. The channel activity of CLIC1 is highly pH dependent (*13, 22*), displaying its lowest activity at pH 7.0 and highest activity at acidic pH values. In this study, the conformational stability of soluble, reduced CLIC1 was investigated as a function of pH in the absence of membranes to improve our understanding of how its conformation might change when the protein encounters the acidic environment at the surface of a membrane. Soluble CLIC1 consists of two structural domains: an N-domain with a thioredoxin-like fold and a C-domain with an all-helical fold. The sequence of α1β2 in the N-domain corresponds to the putative transmembrane region (Figure 1) (*8, 16*). For this region to penetrate a lipid bilayer, the β1α1β2 supersecondary motif will have to detach from the rest of the protein, extend, and refold into its membrane-insertable conformation.

Although the core structure and size of CLIC1 are not significantly altered by pH in the absence of denaturant or membranes, the conformational stability of the native state is diminished at low pH. Equilibrium unfolding data indicate that soluble CLIC1 forms a partially unfolded intermediate which becomes increasingly populated as the pH decreases. Whereas the acid-induced destabilization of many bacterial pore-forming toxins has been reported to form molten globule-like intermediates for membrane insertion (*24, 33*−*37*), the CLIC1 intermediate exhibits significant secondary and tertiary structure with solvent-exposed hydrophobic surfaces and therefore does not fit the definition of a molten globule state. CLIC1 is known to form a dimer under oxidizing conditions that also has an exposed hydrophobic surface (*16*). Since all experiments in this study were performed under reducing

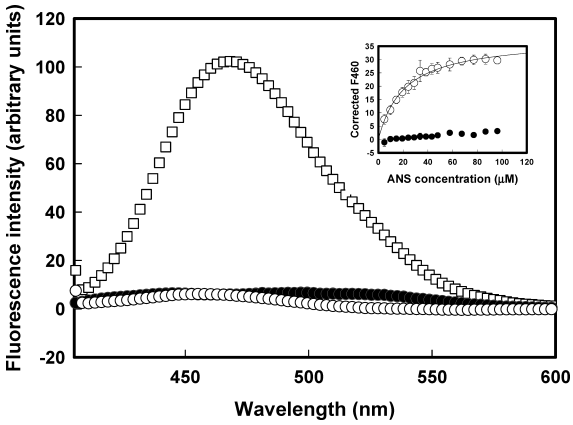

FIGURE 8: Fluorescence emission spectra of ANS at pH 7 (filled) and 5.5 (empty) in the presence of CLIC1 in the native state (● and ○) and the intermediate state (pH 5.5 with 3.8 M urea) (□). Spectra were corrected for the fluorescence of free ANS. The inset shows the isotherms for the binding of ANS to native CLIC1 at pH 7 and 5.5 (●) and to the intermediate state at pH 5.5 with 3.8 M urea (○). The solid line fit yields a K_d of 20 μM for the intermediate.

conditions, it is unlikely that the intermediate species identified here resembles the oxidized dimer, especially in terms of the intramolecular Cys24−Cys59 disulfide bond. However, more detailed structural analysis is required to confirm that there are not other structural similarities. Although the structural details of the N → I transition and how they relate to creating a membrane-insertable form of CLIC1 are currently unknown, Trp35 is involved. Unfolding curves produced by selectively exciting tryptophan (295 nm) show the same trend as those reported in this paper where 280 nm was used as the excitation wavelength, indicating that the fluorescence changes are due to Trp35 and not to Tyr-to-Trp energy transfer. Trp35 is the only tryptophan residue in CLIC1 and is located in helix α1. This amphipathic helix forms the majority of the putative transmembrane region (*2, 8, 10, 13*−*16*) and makes most of the interdomain contacts. To establish whether the sequence corresponding to helix α1 in CLIC1 could form a helix on its own and thereby facilitate membrane insertion, the sequence was analyzed by the AGADIR algorithm which is based on helix−coil transition theory in the absence of tertiary interactions (*56*). The sequence is shown to display a strong propensity to form a helix at both pH 7 and 5.5, suggesting that its helical structure is most likely preserved when the putative transmembrane region inserts into membranes. Compared to those of the C-domain, the greater flexibility and lower stability of the N-domain of GST-like proteins (*57, 58*) most likely facilitate the structural reorganization required to convert the N-domain of soluble CLIC1 to its membrane-insertable conformation.

We propose that the acidic environment encountered by CLICs at the surface of membranes primes the transmembrane region in the N-domain possibly by protonating certain amino acid side chains, thereby lowering the energy barrier for the conversion of soluble CLICs to their membrane-inserted forms. Structural perturbations in proteins due to pH result from changes in the protonation states of titratable residues depending on the pH range (e.g., His, Asp, and Glu at acidic pH). These can alter the electrostatic interactions in the protein structure, giving rise to local or global changes in the stability of the protein and, consequently, its unfolding and refolding characteristics. The amino acid composition of CLIC1 reveals that it has three histidines, 12 aspartates, and 21 glutamates. Inspection of the crystal structure (PDB entry 1K0M) indicates that four of these residues (Glu81, Glu85, Asp225, and Glu228) form hydrogen bonds and salt bridges at the domain interface. These contacts might be significant for maintaining stability, and therefore, protonation changes at these residues could significantly affect the stability of the domain−domain assembly. The role of these residues is currently being investigated. Factors that may trigger the partial unfolding of the acid-destabilized N-domain are the negative potential and low dielectric constant at the membrane surface (*34, 59*).

SUPPORTING INFORMATION AVAILABLE

Three figures as described in the text. This material is available free of charge via the Internet at http://pubs.acs.org.

REFERENCES

1. Chuang, J. Z., Milner, T. A., Zhu, M., and Sung, C. H. (1999) A 29 kDa intracellular chloride channel p64H1 is associated with large dense-core vesicles in rat hippocampal neurons. *J. Neurosci. 19*, 2919–2928.
2. Duncan, R. R., Westwood, P. K., Boyd, A., and Ashley, R. H. (1997) Rat brain p64H1, expression of a new member of the p64 chloride channel protein family in endoplasmic reticulum. *J. Biol. Chem. 272*, 23880–23886.
3. Edwards, J. C. (2000) A novel p64-related Cl^- channel: Subcellular distribution and nephron segment-specific expression. *Am. J. Physiol. 276*, F398–F408.
4. Valenzuela, S. M., Mazzanti, M., Tonini, R., Qui, M. R., Warton, K., Musgrove, E. A., Campbell, T. J., and Breit, S. N. (2000) The nuclear chloride ion channel NCC27 is involved in regulation of the cell cycle. *J. Physiol. 529*, 541–552.
5. Ulmasov, B., Bruno, J., Woost, P. G., and Edwards, J. C. (2007) Tissue and subcellular distribution of CLIC1. *BMC Cell Biol. 8*, 8.
6. Ashley, R. H. (2003) Challenging accepted ion channel biology: p64 and the CLIC family of putative intracellular anion channel proteins. *Mol. Membr. Biol. 20*, 1–11.
7. Dulhunty, A., Gage, P., Curtis, S., Chelvanayagam, G., and Board, P. (2001) The glutathione transferase structural family includes a nuclear chloride channel and a ryanodine receptor calcium release channel modulator. *J. Biol. Chem. 276*, 3319–3323.
8. Harrop, S. J., De Maere, M. Z., Fairlie, W. D., Rezstsova, T., Valenzuela, S. M., Mazzanti, M., Tonini, R., Qiu, M. R., Jankova, L., Warton, K., Bauskin, A. R., Wu, W. M., Pankhurst, S., Campbell, T. J., Breit, S. N., and Curmi, P. M. G. (2001) Crystal structure of a soluble form of the intracellular chloride ion channel CLIC1 (NCC27) at 1.4 Å resolution. *J. Biol. Chem. 276*, 44993–45000.
9. Littler, D. R., Assaad, N. N., Harrop, S. J., Brown, L. J., Pankhurst, G. J., Luciani, P., Aguilar, M. I., Mazzanti, M., Berryman, M. A., Breit, S. N., and Curmi, P. M. (2005) Crystal structure of the soluble form of the redox-regulated chloride ion channel protein CLIC4. *FEBS J. 272*, 4996–5007.
10. Berry, K. L., and Hobert, O. A. (2006) Mapping functional domains of chloride intracellular channel (CLIC) proteins in vivo. *J. Mol. Biol. 359*, 1316–1333.
11. Cromer, B. A., Gorman, M. A., Hansen, G., Adams, J. J., Coggan, M., Littler, D. R., Brown, L. J., Mazzanti, M., Breit, S. N., Curmi, P. M. G., Dulhunty, A. F., Board, P. G., and Parker, M. W. (2007) Structure of the Janus protein human CLIC2. *J. Mol. Biol. 347*, 719–731.
12. Littler, D. R., Harrop, S. J., Brown, L. J., Pankhurst, G. J., Mynott, A. V., Luciani, P., Mandyam, R. A., Mazzanti, M., Tanda, S., Berryman, M. A., Breit, S. N., and Curmi, P. M. G. (2008) Comparison of vertebrate and invertebrate CLIC proteins: The crystal structures of *Caenorhabditis elegans* EXC-4 and *Drosophila melanogaster* DmCLIC. *Proteins 71*, 364–378.

13. Warton, K., Tonini, R., Fairlie, W. D., Mathews, J. M., Valenzuela, S. M., Qiu, M. R., Wu, W. M., Pankhurst, S., Bauskin, A. R., Harrop, S. J., Campbell, T. J., Curmi, P. M. G., Breit, S. N., and Mazzanti, M. (2002) Recombinant CLIC1 (NCC27) assembles in lipid bilayers via a pH-dependent two-state process to form chloride ion channels with identical characteristics to those observed in Chinese hamster ovary cells expressing CLIC1. *J. Biol. Chem. 277*, 26003–26011.
14. Singh, H., and Ashley, R. H. (2006) Redox regulation of CLIC1 by cysteine residues associated with the putative channel pore. *Biophys. J. 90*, 1628–1638.
15. Berry, K. L., Bülow, H. E., Hall, D. H., and Hobert, O. A. (2003) A *C. elegans* CLIC-like protein required for intracellular tube formation and maintenance. *Science 302*, 2134–2137.
16. Littler, D. R., Harrop, S. J., Fairlie, D., Brown, L. J., Pankhurst, G. J., Pankhurst, S., DeMaere, M. Z., Campbell, T. J., Bauskin, A. R., Tonini, R., Mazzanti, M., Breit, S. N., and Curmi, P. M. G. (2004) The intracellular chloride ion channel protein CLIC1 undergoes a redox-controlled structural transition. *J. Biol. Chem. 279*, 9298–9305.
17. Tulk, B. M., and Edwards, J. C. (1998) NCC27, a homologue of intracellular chloride channel p64, is expressed in brush border of renal proximal tubule. *Am. J. Physiol. 274*, F1140–F1149.
18. Tonini, R., Ferroni, A., Valenzuela, S. M., Warton, K., Campbell, T. J., Breit, S. N., and Mazzanti, M. (2000) Functional characterisation of the NCC27 nuclear protein in stable transfected CHO-K1 cells. *FASEB J. 14*, 1171–1178.
19. White, S. H., and Wimley, W. C. (1999) Membrane protein folding and stability: Physical principles. *Annu. Rev. Biophys. Biomol. Struct. 28*, 319–365.
20. Parker, M. W., and Feil, S. C. (2005) Pore-forming protein toxin: From structure to function. *Prog. Biophys. Mol. Biol. 88*, 91–142.
21. Singh, H., and Ashley, R. H. (2007) CLIC4 (p64H1) and its putative transmembrane domain form poorly selective, redox-regulated ion channels. *Mol. Membr. Biol. 24*, 41–52.
22. Tulk, B. M., Kapadia, S., and Edwards, J. C. (2002) CLIC1 inserts from the aqueous phase into phospholipid membranes, where it functions as an anion channel. *Am. J. Physiol. 282*, C1103–C1112.
23. McLaughlin, S. (1989) The electrostatic properties of membranes. *Annu. Rev. Biophys. Biophys. Chem. 18*, 113–136.
24. Van der Goot, F. G., González-Manãs, J. M., Lakey, J. H., and Pattus, F. (1991) A 'molten-globule′ membrane-insertion intermediate of the pore-forming domain of colicin A. *Nature 354*, 408–410.
25. Bortoleto, R. K., and Ward, R. J. (1999) A stability transition at mildly acidic pH in the α-hemolysin (α toxin) from *Staphylococcus aureus*. *FEBS Lett. 459*, 438–442.
26. Manceva, S. D., Pusztai-Carey, M., and Butko, P. (2004) Effect of pH and ionic strength on the cytolytic toxin Cyt1A: A fluorescence spectroscopy study. *Biochim. Biophys. Acta 1699*, 123–130.
27. Parker, M. W., and Pattus, F. (1993) Rendering a membrane protein soluble in water: A common packing motif in bacterial protein toxins. *Trends Biochem. Sci. 18*, 391–395.
28. London, E. (1992) Diphtheria toxin: Membrane interaction and membrane translocation. *Biochim. Biophys. Acta 1113*, 25–51.
29. Lacy, D. B., and Stevens, R. C. (1998) Unravelling the structures and modes of action of bacterial toxins. *Curr. Opin. Struct. Biol. 6*, 778–784.
30. Zakharov, S. D., and Cramer, W. A. (2002) Colicin crystal structures: Pathways and mechanisms for colicin insertion into membranes. *Biochim. Biophys. Acta 1565*, 333–346. Li, Y. F., Li, D. F., Zang, Z. H., and Wang, D. C. (2006) Trimeric structure of the wild soluble chloride intracellular ion channel CLIC4 observed in crystals. *Biochem. Biophys. Res. Commun. 1565*, 333–346.
31. Thuduppathy, G. R., and Hill, R. B. (2006) Acid destabilisation of the solution conformation of Bcl-$_{XL}$ does not drive its pH-dependent insertion into membranes. *Protein Sci. 15*, 1–10.
32. Gong, X. M., Choi, J., Franzin, C. M., Zhai, D., Reed, J. C., and Marassi, F. M. (2004) Conformation of membrane associated proapoptotic tBid. *J. Biol. Chem. 279*, 28954–28960.
33. Blewitt, M. G., Chung, L. A., and London, E. (1985) Effect of pH on the conformation of diphtheria toxin and its implications for membrane penetration. *Biochemistry 24*, 5458–5464.
34. Bychkova, V. E., Dujsekina, A. E., Kleni, S. I., Tiktopulo, E. I., Uversky, V. N., and Ptitsyn, O. B. (1996) Molten globule-like state of cytochrome c under conditions simulating those near the membrane surface. *Biochemistry 35*, 6058–6063.
35. Chenal, A., Savarin, P., Nizard, P., Guillain, F., Gillet, D., and Forge, V. (2002) Membrane protein insertion regulated by bringing electrostatic and hydrophobic interactions into play: A case study with the translocation domain of the diphtheria toxin. *J. Biol. Chem. 277*, 43425–43432.
36. Song, J., Bai, P., Luo, L., and Peng, Z. Y. (2001) Contribution of individual residues to the formation of the native-like tertiary topology in the formation of the α-lactalbumin molten globule. *J. Mol. Biol. 280*, 167–174.
37. Prats, M., Teissie, J., and Tocanne, J.-F. (1986) Lateral proton conduction at lipid-water interfaces and its implication for the chemiosmotic coupling hypothesis. *Nature 322*, 756–758.
38. Lesieur, C., Vecsey-Semjen, B., Abrami, L., Fivaz, M., and Gisou van der Goot, F. (1997) Membrane insertion: The stratergies of toxins. *Mol. Membr. Biol. 14*, 45–64.
39. Thuduppathy, G. R., Craig, J. W., Kholodenko, V., Schon, A., and Hill, B. (2006) Evidence that membrane insertion of the cytosolic domain of Bcl-$_{XL}$ is governed by an electrostatic mechanism. *J. Mol. Biol. 359*, 1045–1058.
40. Thuduppathy, G. R., Terrones, O., Craig, J. W., Basanez, G., and Hill, R. B. (2006) The N-terminal domain of BCL-XL reversibly binds membranes in a pH-dependent manner. *Biochemistry 45*, 14533–14542.
41. Valenzuela, S. M., Martin, D. K., Por, S. B., Robbins, J. M., Warton, K., Bootcov, M. R., Schofield, P. R., Campbell, T. J., and Breit, S. N. (1997) Molecular cloning and expression of a chloride ion channel of cell nuclei. *J. Biol. Chem. 272*, 12575–12582.
42. Beecham, J. M. (1992) Global analysis of biochemical and biophysical data. *Methods Enzymol. 210*, 37–54.
43. Zitzewitz, J. A., Bilsel, O., Luo, J., Jones, B. E., and Matthews, C. R. (1995) Probing the folding mechanism of a leucine zipper peptide by stopped flow circular dichroism spectroscopy. *Biochemistry 34*, 12812–12819.
44. Bilsel, O., Zitzewitz, J. A., Bowers, K. E., and Matthews, C. R. (1999) Folding mechanism of the α-subunit of tryptophan synthase, an α/β barrel protein: Global analysis highlights the interconversion of multiple native, intermediate and unfolded forms through parallel channels. *Biochemsitry 38*, 1018–1029.
45. Pace, C. N. (1973) Urea and guanidine hydrochloride denaturation of ribonuclease, lysozyme, α-chymotrypsin and β-lactoglobulin. *J. Biol. Chem. 249*, 5388–5393.
46. Pace, C. N. (1986) Determination and analysis of urea and guanidine hydrochloride denaturation curves. *Methods Enzymol. 131*, 266–280.
47. Semisotnov, G. V., Rodionova, N. A., Razgulyaev, O. I., Uversky, V. N., Gripas, A. F., and Gilmanshin, R. I. (1991) Study of the "molten globule" intermediate state in protein folding by a hydrophobic fluorescence probe. *Biopolymers 31*, 119–128.
48. Stryer, L. (1965) The interaction of a naphthalene dye with apomyoglobin and apohemoglobin. A fluorescent probe of non-polar binding sites. *J. Mol. Biol. 13*, 482–495.
49. Ptitsyn, O. B. (1995) Molten globule and protein folding. *Adv. Protein Chem. 47*, 83–229.
50. Fink, A. L. (1995) in *Methods in Molecular Biology, Volume 40: Protein Stability and Folding: Theory and Practice* (Shirley, B. A., Ed.) pp 343−360, Humana Press Inc., Totowa, NJ.
51. Kuwajima, K. (1989) The molten globule state as a clue for understanding the folding and cooperativity of globular-protein structure. *Proteins 6*, 87–103.
52. Chamberlain, A. K., and Marqusee, S. (1998) Molten globule unfolding monitored by hydrogen exchange in urea. *Biochemistry 37*, 1736–1742.
53. Jamin, M., Antalik, M., Loh, S. N., Bolen, D. W., and Baldwin, R. L. (2000) The unfolding enthalpy of the pH 4 molten globule of apomyoglobin measured by isothermal titration calorimetry. *Protein Sci. 9*, 1340–1346.
54. Bailey, R. W., Dunker, A. K., Brown, C. J., Garner, E. C., and Griswold, M. D. (2001) Clusterin, a binding protein with a molten globule-like region. *Biochemistry 40*, 11828–11840.
55. Banerjee, T., and Kishore, N. (2005) 2,2,2-Trifluoroethanol-Induced Molten Globule State of Concanavalin A and Energetics of 8-Anilinonaphthalene Sulfonate Binding: Calorimetric and Spectroscopic Investigation. *J. Phys. Chem. B 109*, 22655–22662.
56. Lacroix, E., Viguera, A. R., and Serrano, L. (1998) Elucidating the folding problem of α helices: Local motifs, long range electrostatics, ionic strength, dependence and prediction of NMR parameters. *J. Mol. Biol. 284*, 173–191.
57. Dragani, B., Iannarelli, V., Allocati, N., Masulli, M., Cicconetti, M., and Aceto, A. (1998) Irreversible thermal denaturation of

glutathione transferase P1-1. Evidence for varying structural stability of different domains. *Int. J. Biochem. Cell Biol. 30*, 155–163.
58. Thompson, L. C., Walters, J., Burke, J., Parsons, J. F., Armstrong, R. N., and Dirr, H. W. (2006) Double mutation at the subunit interface of glutathione transferase rGSTM1-1 results in a stable, folded monomer. *Biochemistry 45*, 2267–2273.
59. Endo, T., and Schatz, G. (1988) Latent membrane perturbation activity of a mitochondrial precursor protein is exposed by unfolding. *EMBO J. 7*, 1153–1158.
60. DeLano, W. L. (2004) PyMol, DeLano Scientific, San Carlos, CA.

BI801147R